Available online at www.sciencedirect.com

SciVerse ScienceDirect

Ceramics International 39 (2013) 4339–4347

CERAMICS INTERNATIONAL

www.elsevier.com/locate/ceramint

Synthesis and *in-vitro* cytotoxicity analysis of microwave irradiated nano-apatites

Rabia Nazir[1,a], Abdul Samad Khan[a,*,1], Aftab Ahmed[b], Anis Ur-Rehman[c], Aqif Anwar Chaudhry[a], Ihtesham Ur Rehman[d], Ferranti S.L. Wong[e]

[a]*Interdisciplinary Research Centre in Biomedical Materials, COMSATS Institute of Information Technology, Lahore, Pakistan*
[b]*School of Biological Sciences, University of the Punjab, Lahore, Pakistan*
[c]*Department of Physics, COMSATS Institute of Information Technology, Islamabad, Pakistan*
[d]*Department of Material Science and Engineering, The Kroto Research Institute, University of Sheffield, Sheffield, United Kingdom*
[e]*Paediatric Dentistry, Centre for Oral Growth and Development, Barts and the London School of Medicine and Dentistry, Queen Mary University of London, London, United Kingdom*

Received 26 September 2012; received in revised form 6 November 2012; accepted 8 November 2012
Available online 5 December 2012

Abstract

Nano-sized calcium deficient apatite (CDA) micelles were synthesized through microwave assisted the wet precipitation technique. Cetyltrimethylammonium bromide (CTAB) was employed as surface template to furnish the CDA particles with tailored size and shape. As-precipitated CDA was heat treated to observe the effect of heat treatment temperature on the interatomic rearrangement of entities within the apatite lattice. This transformation is responsible for conversion of CDA to β-tricalcium phosphate (β-TCP) at specific temperature. The phase purity, particles size, morphology and transformation kinetics were analyzed using X-ray Diffraction (XRD), Fourier Transform Infrared Spectroscopy (FTIR), Scanning Electron Microscopy (SEM) and Thermogravimetric Analysis (TGA). *In-vitro* studies were performed on β-TCP with three cell lines: osteoblasts, HeLa, and SF 767. The results showed that nano-sized particles were successfully synthesized in short time. The cells had appreciable proliferation/attachment on the surface of these nano-particles. It is concluded that the microwave irradiated synthesized β-TCP has good capacity in terms of biocompatibility and has the potential to be used in hard tissue regeneration applications.

Keywords: Tricalcium phosphate (TCP); Microwave assisted synthesis; Nano-particles; Cytotoxicity

1. Introduction

Calcium phosphate (CP) family is known for hard tissue (enamel, dentin and bone) replacement and regeneration due to its similarity to the biological apatite [1,2]. Hydroxyapatite [HA, $Ca_{10}(PO_4)_6(OH)_2$], tri-calcium phosphate [TCP, $Ca_3(PO_4)_2$] and tetra calcium phosphate [TTCP, $Ca_4P_2O_9$] are well known calcium phosphates [3]. Over the last few decades, CPs have been used for bone regeneration, dental restorations, maxillofacial implants and scaffolds for tissue engineering are examples of biomedical applications [4,5]. The difference in biological performance of different calcium phosphates is attributed to the difference in their stoichiometry. Hydroxyapatite (HA) with calcium to phosphate (Ca/P) molar ratio 1.67 is calcium enriched apatite that shows stability in physiological fluids. However, bone mineral is essentially calcium deficient apatite (CDA) with Ca/P molar ratio 1.5 which is stoichiometrically identical to TCP and structurally to HA [6]. CDA generally has higher surface area as compared to HA hence it facilitates improved bioactivity for the formation of apatite layer on its surface [7].

Several techniques are in practice for the synthesis of calcium phosphate apatites such as the wet precipitation

*Correspondence to: Dental Materials Interdisciplinary Research Centre in Biomedical Materials, COMSATS Institute of Information Technology, Defence Road, Off Raiwind Road, Lahore, Pakistan. Tel.: +92 3325426230; fax: +92 429203100.
E-mail address: draskhan@ciitlahore.edu.pk (A. Samad Khan).
[1]Both authors contributed equally to this work.

0272-8842/$ - see front matter © 2012 Elsevier Ltd and Techna Group S.r.l. All rights reserved.
http://dx.doi.org/10.1016/j.ceramint.2012.11.017

[8], solid state synthesis [9], sol–gel synthesis [10] and hydrothermal techniques [11]. However these techniques have certain limitations e.g. wet precipitation requires prolonged reaction times while hydrothermal and sol–gel require expensive chemicals. Microwave assisted synthesis approach (both solid and wet) has been recently used for the preparation of wide range of materials (composites, polymers and ceramics) [12]. The technique furnishes the product in much shorter time with high purity. Synthesis of nano-structured CP by microwave assisted wet precipitation has been reported in literature [13,14]. However previous studies [13,15] related to microwave assisted synthesis suggested a longer exposure time which is a waste of useful energy.

Synthesis of surface-modified nano-structured ceramics using different surfactants has also been reported. Sodium sulfide (Na_2S) has been used for the synthesis of nano-structured wires/rods of silver [16]. Similarly pyridine and Cetyltrimethylammonium bromide (CTAB) has been used for tailoring the structure of ZnO and Bi_2S_3 respectively [17,18]. Various surfactants such as mixed poly(oxyethylene)nonyl phenol ether (NP5), poly(oxyethylene)nonyl phenol ether (NP9) [19] and micro-emulsion environments facilitated by W/O (water in oil) [20] have been used for synthesis of apatites. CTAB, anionic surfactant with antibacterial properties, has been found to stimulate the nano structure of different materials [18,21]. This is due to the fact that CTAB has been known to produce stable atomic clusters with tailorable microstructures depending upon the experimental parameters [21].

Satisfactory cytotoxicity and biocompatibility of synthetic HA and TCP has been frequently reported in literature [22–24]. The biocompatibility and their tissue response depend on the certain factors i.e. chemical composition, surface texture, shape, and size. It is difficult to analyze the *in-vivo* response of biomaterials because numerous cells are involved during this process therefore; *in-vitro* methods are useful in evaluating cell interactions with biomaterials. Therefore the aim of this study was to optimize the condition of synthesizing CDA in shortest possible time while using surfactants and to elucidate the interaction of these apatites with various types of cells.

2. Materials and methods

Analytical grade calcium nitrate ($Ca(NO_3)_2 \cdot 4H_2O$) (UniChem, Pak) and diammonium hydrogen phosphate ($(NH_4)_2HPO_4$) (AppliChem, Germany) were used as precursors for the synthesis of CDA. 1 M ($Ca(NO_3)_2 \cdot 4H_2O$) and 0.6 M ($(NH_4)_2HPO_4$) solutions were prepared in water and ethanol respectively with initial Ca/P molar ratio of 1.5. CTAB (5% of theoretical yield of CDA) was added as surfactant to phosphorous precursor and pH of both solutions was maintained at 9 by adding ammonium hydroxide (BDH, UK). [$(NH_4)_2HPO_4$] solution was added drop wise to [$(Ca(NO_3)_2 \cdot 4H_2O$] solution at a dropping rate of 2 ml min^{-1}. The reaction mixture was then stirred for 30 min (pH maintained at 9) before refluxing in a domestic microwave oven (Samsung MW101P) at1000 W for 3 min. After microwave irradiation the resulting reaction mixture was filtered, washed with distilled water and aged in drying oven at 80 °C for 22 h. The resulting powder was heat treated at 400, 600, 800 and 1000 °C for 1 h (ramp rate ≈ 10 °C min^{-1}) and cooled down to room temperature (ramp rate ≈ 30 °C min^{-1}). Resulting products were isolated and characterized by using Fourier Transform Infrared Spectroscopy (FTIR), X-ray Diffraction (XRD), Thermogravimetric Analysis (TGA), and Scanning Electron Microscope (SEM). The biocompatibility of the samples was characterized by cell-culturing.

2.1. Samples preparation:

Five discs of TCP HT 1000 °C were pressed into cylindrical discs (5×2 mm^2) by using hydraulic press (650 Psi, 10 s) stainless steel die (5 mm dia). These samples were utilized for cell culturing studies after sterilizing by autoclaving.

2.2. Characterization

2.2.1. Fourier Transform Infrared Spectroscopy (FTIR):

Characteristic functional groups were identified using Fourier Transform Infrared (FTIR, Nicolet 6700, USA) Spectroscopy. Photoacoustic cell was used as detector. Spectra were collected over the region 4000–400 cm^{-1} at resolution of 4 cm^{-1} averaging 256 scans.

2.2.2. X-ray Diffraction (XRD):

X-ray diffraction (XRD) technique was used to evaluate phase transformation in CDA. Analysis was carried out on diffractometer system PERT-PRO using Goniometer geometry (PW3050/60) at room temperature with Cu K-α radiation. XRD pattern was recorded continuously with 2⊖ from 20° to 80°with a step size of 0.02°.

2.2.3. Thermogravimetric Analysis (TGA):

Thermogravimetric analysis (TGA) was performed on QEX-600 using platinum pan as reference material. Analysis was carried out between 20°–1200 °C at the rate of 20 °C min^{-1} under inert nitrogen environment.

2.2.4. Scanning Electron Microscopy (SEM):

Powder morphology and particle size was investigated by Scanning Electron Microscope (JEOL JSM6490A, Japan) at a voltage of 20 V. Samples were gold coated in a vacuum (thickness ≈ 250 Å) using JFC 1500 Ion sputtering device. Images were taken in the magnification range from 25× to 50× operated at accelerated voltage of 20 KV.

2.2.5. Cell culturing

2.2.5.1. Osteoblast cells. Ethical permission was taken from Institutional ethical committee prior to testing. For

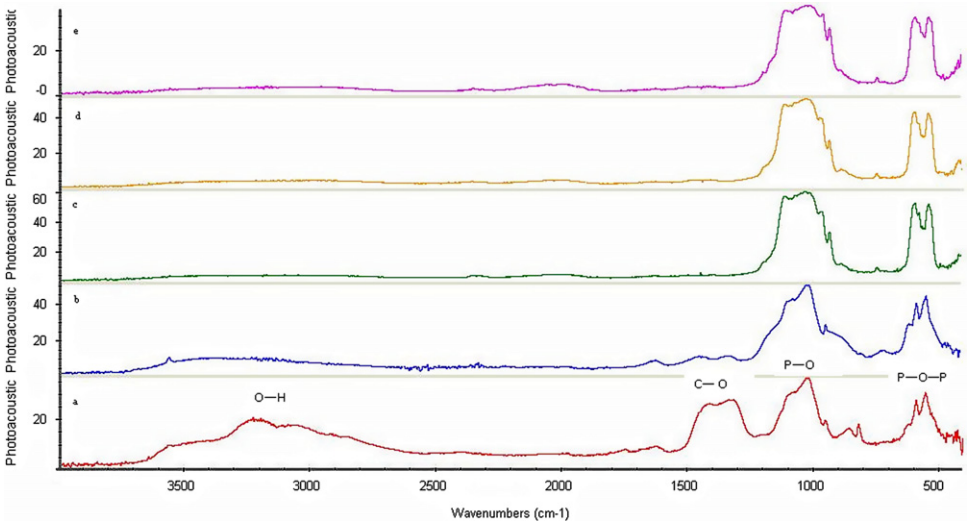

Fig. 1. FTIR spectra of (a) as precipitated, [calcium deficient apaptite: (b) HT400 °C, (c) HT600 °C, (d) HT800 °C, and (e) HT1000 °C].

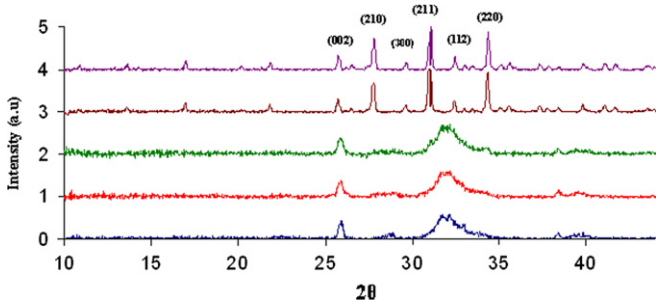

Fig. 2. XRD pattern of (a) As precipitated, [calcium deficient hydroxyapatite (b) HT400 °C, (c) HT600 °C, (d) HT800 °C, and (e) HT1000 °C].

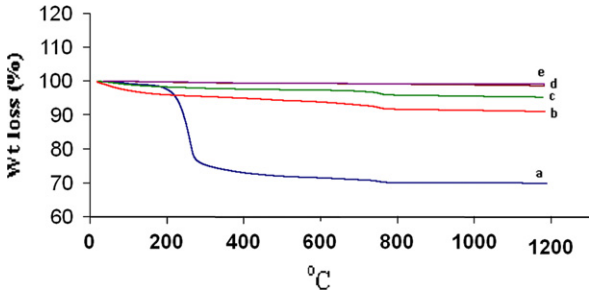

Fig. 3. TGA graphs of (a) as-precipitated (b) 400 °C, (c) 600 °C, (d) 800 °C, and (e) 1000 °C showing weight loss behavior up to 1200 °C.

the isolation of osteoblast [fetal calvarial cells (FCCs)] 18th day pregnant mice was sacrificed by cervical dislocation. Mouse was dissected and uterus was isolated. The fetus was isolated into petri dish and washed several times with PBS. Head region was separated and brain was extracted. The calvarial region was washed and finally cut it into small pieces to dissociate the cells. Dulbecco's modified eagle medium (DMEM) was added and the cells were re-suspended by passing them through a needle (5 cc syringe) several times. When cells were dissociated from each other, cells were spun at 1800 rpm for 5 min in a centrifuge (Eppendorf 5415R-Germany). The pellet was suspended in complete medium and the numbers of cells were counted by hemocytometer (Neubauer, Germany). The cells were added in culture flask and incubated at 37 °C with 5% in CO_2 in humid environment (Memmert-Germany).

In this procedure, 3×10^4 FCCs were added in each well of 12 well plate (NUNC) followed by addition of experimental samples respectively in 1 ml complete medium. Cells were allowed to grow for 3 days at 37 °C with 5% CO_2 in a humidified environment and digital images were taken. Cells were also stained by trypan blue and images of cells were taken by inverted microscope (Olympus IX51-USA). In addition cells were trypsinized and counted the number of control (polystyrene well plate) and experimental samples (β-TCP) treated cells after 3 and 7 days of growth were counted. All the experiments were done in triplicates.

2.2.5.2. HeLa and SF767 cells. In this study, 3×10^4 HeLa cells were added in 12 well plate (NUNC) containing 1 ml medium Dulbecco's modified eagle medium (DMEM containing glutamine, 10% fetal bovine serum (FBS), 100 μg/ml penicillin, and 100 μg/ml streptomycin). Five sterilized discs of TCP were added to the well immediately and the wells were labeled accordingly. Similarly 3×10^4 SF767 cells were added in 12 well plate in 1 ml medium and sterile discs were added and labeled. The cells were incubated at 37 °C with 5% CO_2 in humidified environment for 7 days with medium change after 3 days. After 7 days of incubation, images of cells were taken (bright field microscopy, Olympus IX51-USA). Cells were stained with trypan blue and crystal violet and images were taken respectively. In addition total number of cells was counted on control (polystyrene well plate) and experimental samples (β-TCP) containing wells by hemocytometer. All the experiments were done in triplicates.

3. Results

3.1. Fourier Transform Infrared Spectroscopy (FTIR)

FTIR spectra of as-precipitated CDA and heat treated samples at 400 °C, 600 °C, 800 °C and 1000 °C are shown in Fig. 1(a–e respectively). In as-precipitated spectrum the broad band in the range 3100–3400 $cm^{-1}$and at 1640 cm^{-1} were corresponded to adsorbed water. Peaks at 1455 cm^{-1} and 1402 cm^{-1} were assigned to adsorbed CO_3^{-2} ions on the surface. In addition, presence of CDA was confirmed by the characteristic phosphate bands at 1100, 1031, 875, 600–550 and 470 cm^{-1}. Peaks at 1100 and 1031 cm^{-1} were assigned to triply degenerated (υ_3) asymmetric stretching mode of P–O bond. The 875 cm^{-1} band indicated non-degenerated (υ_1) P–O symmetric stretching mode. Peaks at 602 and 564 cm^{-1} revealed presence of triply degenerated (υ_4) bending mode of P–O–P bond. The broader phosphate bands around 1031and 564 cm^{-1} (υ_3 and υ_4 respectively) indicated amorphous nature of as-synthesized CDA. It was observed that in heat treated samples peaks at 1100 and 1031 cm^{-1} substantially became well defined as temperature increased from 400 to 1000 °C. New peak appeared at 960 cm^{-1} in heat treated sample at 600 °C which was assigned to the non-degenerated (υ_1) P–O symmetric stretching mode. Similarly, the peak at 602 cm^{-1} showed an increase in peak height due to increase in crystallinity, however, the neighboring peak at 564 cm^{-1} did not show any change. Increase in temperature beyond 800 °C did not show any significant phase transformation, however, there was a slight increase in crystallinity when heat treated at 800–1000 °C. It clearly showed that transformation of CDA to β-TCP was completed up to 800 °C.

3.2. X-ray Diffraction (XRD)

Crystallographic identification of the phases of the synthesized CDA and heat treated samples at 400 °C, 600 °C 800 °C and 1000 °C are given in Fig. 2. The phases were identified by comparing the experimental XRD patterns to standards compiled by the Joint Committee on Powder Diffraction Standards (ICDD) using card numbers: 46-0905 for CDHA, 09-0169 and 70-2065 for β-TCP [2]. The broad peaks in the XRD pattren of as-synthesized CDA at 26.03 (002) and 32.15 (211) indicated amorphous nature of apatite.

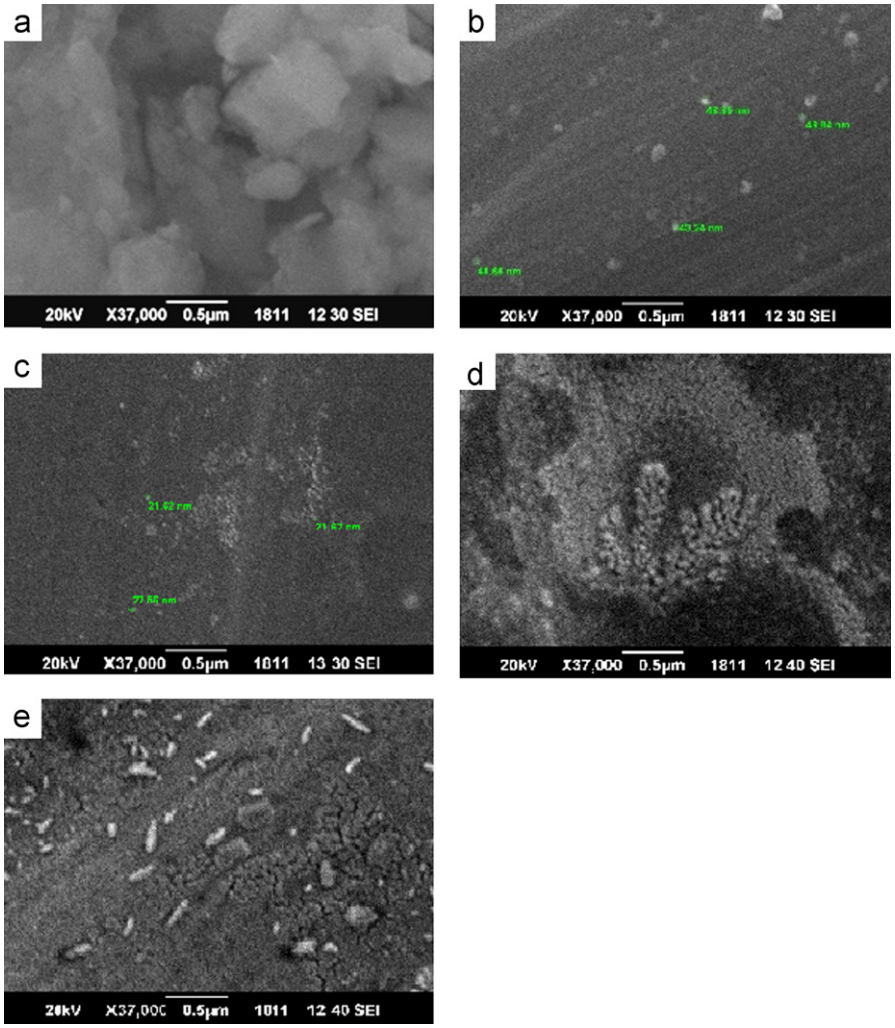

Fig. 4. Scanning Electron Micrographs of (a) as-precipitated CDHA, (b) HT400 °C, (c) HT600 °C, (d) HT800 °C, and (e) HT1000 °C.

The change in the pattren of CDA upto 600 °C was not significant, however, peaks at 26.03 (002) and 32.15 (211) were broadened slightly at 600 °C as compared to that of 400 °C. This was due to burn out of CTAB which eliminated around 500 °C [22]. At 800 °C, peaks shape changed from broad to narrow. Sharp and well defined peaks at 26.03 (002), 32.15 (211) and 32.48 (112) showed the behavior of increase in crystallite size and crystallinity. New peaks appeared at 27.84 (210), 34.40 (220) and 29.77 (300) which indicated transformation of CDA to β-TCP. This result is in complete agreement with FTIR results which also showed change in this range of temperature. No further change in β-TCP structure up to 1000 °C was observed. No impurities were found in the XRD patterns.

3.3. Thermogravimetric Analysis (TGA)

Temperature–weight loss profiles (TGA graphs) of as-precipitated CDA and heat treated samples at 400 °C, 600 °C 800 °C and 1000 °C are shown in Fig. 3. As-precipitated CDA showed weight loss of almost 30% in this temperature range. Significant weight loss was observed up to 270 °C. During the experimental reaction ammonium nitrate (NH_4NO_3) was obtained as by-product. Removal of NH_4NO_3 (M.P. ≈ 170 °C) may partly contribute to the weight loss up to 200 °C. Weight loss observed between 200–280 °C was due the removal of physical adsorbed water. The gradual weight loss in the temperature range 300–750 °C was due to the slow decomposition of the CDA into β-TCP given by following equation:

$$Ca_9HPO_4(PO4)_5OH \rightarrow 3Ca_3(PO_4)_2 + H_2O$$

In addition, weight loss in this temperature range might be due to the elimination of CTAB at 500 °C. The powder heat treated at 400 °C showed almost 10% weight loss. This weight loss represented the removal of chemically combined water as well as trace amounts of physically combined water and CTAB. As the powder was heat treated at higher temperature (400 °C–600 °C) amount of weight loss was reduced to less than 3% (due to the moisture removal). No weight loss was observed in the heat treated powder (800 °C and 1000 °C) up to 1200 °C which confirmed their thermal stability.

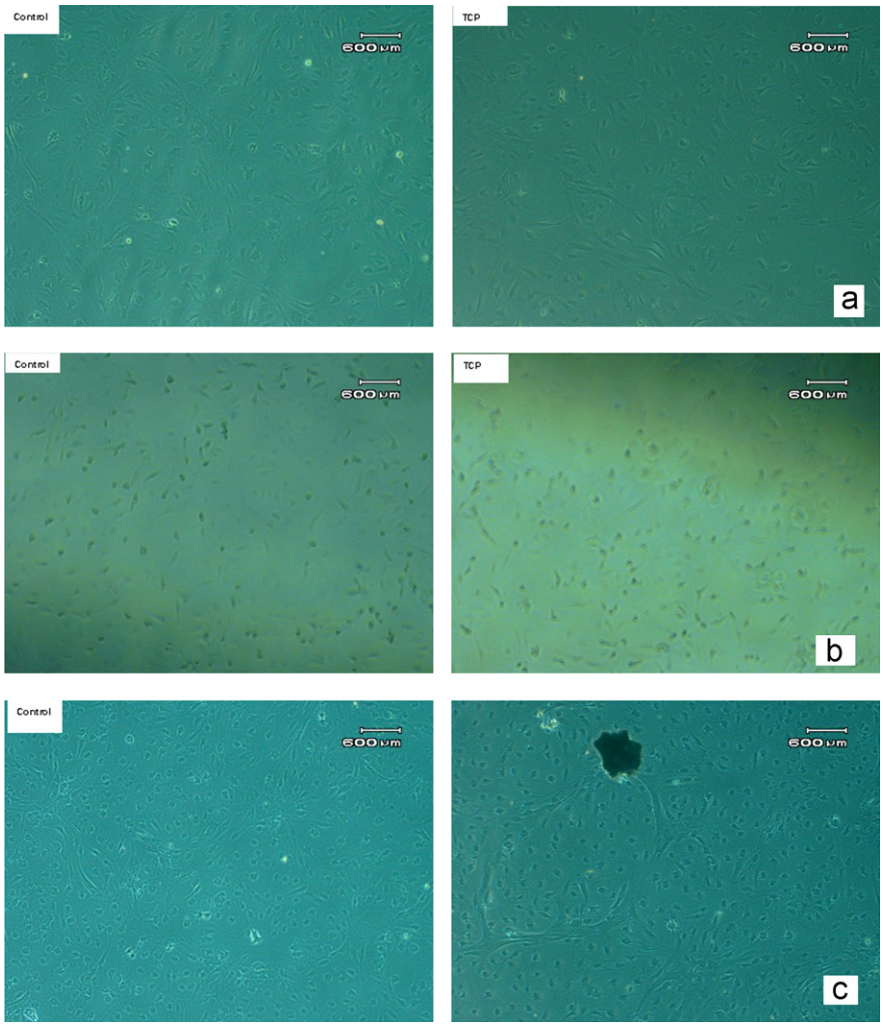

Fig. 5. (a) Images of FCCs after trypan blue staining. (b) Bright field images of FCCs after 7 days of growth of control and biomaterial treated cells. (c) Images of FCCs after trypan blue staining after 7 days of culture.

3.4. Scanning Electron Microscopy (SEM)

SEM micrographs of as precipitated CDA, heat treated CDA at 400 °C, 600 °C, 800 °C and 1000 °C are shown in Fig. 4 respectively. The morphological pattern showed that particle size was in 20–50 nm range. The individual particles tended to agglomerate and sinter when temperature was raised to 800 °C and degree of agglomeration was further increased at 1000 °C. The increase in temperature provides the driving force for particulate coalescence. In addition, the particle morphology is spherical which is highly desirable in bioactive dental fillers.

3.5. Cell culturing

3.5.1. Osteoblast cells (FCCs)

There was no apparent change in morphology of control and TCP treated cells (black spot in the images are contents of TCP), there was no change in morphology of cells even which were in direct contact with TCP which indicated that material was not toxic for cells. The cell proliferation results on day 7 showed that there was continuous growth of cells on all experimental samples and significant difference was observed ($p \leq 0.05$), however, the growth rate was higher for control [75,000 (S.D $\pm$ 4242.65)] as compared to TCP samples [58,000 (S.D $\pm$ 2000)]. After staining the cells with trypan blue, no darkly stained blue cells were observed in control and TCP treated cells. This clearly indicated that there was no death in TCP treated osteoblasts. From the results it appeared that for the initial few days cells adopted to grow in the presence of TCP and later they started proliferation (Fig. 5b and c).

3.5.2. HeLa cells

All samples (control and TCP samples) contained equal number of cells on day 0 (30,000/well) for each group of cells. The cell proliferation results for HeLa cells after 7 days showed that there was continuous growth of cells in all experimental samples. The growth pattern of cells were

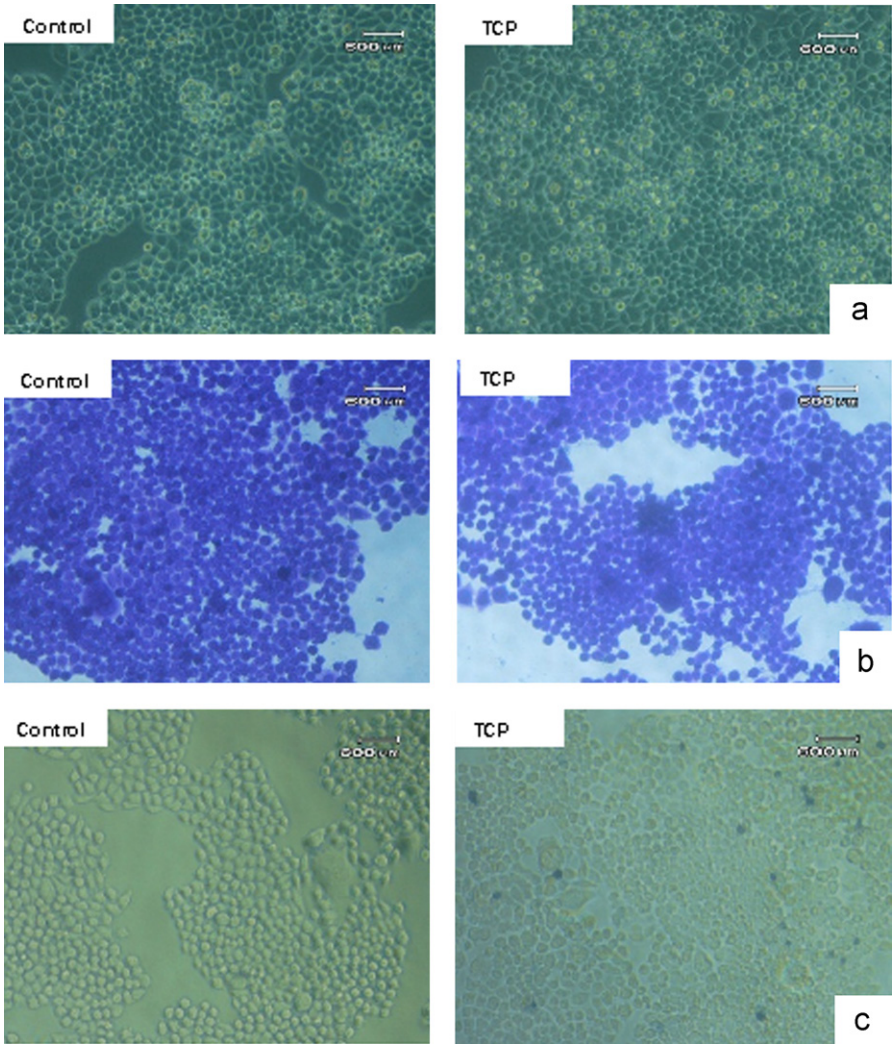

Fig. 6. (a) Bright field images of HeLa cells taken after 7 days of growth; (b) images of HeLa cells after Crystal Violet Staining (C.V.); (c) images of cells after trypan blue staining.

statistically significant ($p \leq 0.05$), however the cell count was slightly higher for TCP samples [360,000 (S.D $\pm$ 3000) than control samples 345,000 (S.D $\pm$ 7071). Morphological images were taken of these cells for 7 days are shown in Fig. 6. Cells were colonized and the findings corresponded to continuous proliferation. When cells were stained with trypan blue after 7 days in culture both experimental and control samples, it was observed that for control group there was not a single cell stained blue whereas, 19 (TCP) cells/observed area (insignificant) were stained blue which indicated some level of death in cells which were grown in the presence of TCP (Fig. 6b and c).

3.5.3. SF-767 cells

Cell count for both control and TCP samples was the same as for HeLa cells on day 0 (30,000). The cell proliferation results showed that there was continuous growth of cells after 7 days however insignificant difference was observed between control [236,000 (S.D $\pm$ 5657)] and TCP [210,000 (S.D $\pm$ 2000)]. The morphological pattern (Fig. 7a) of all these samples was same that showed the colony formation and attributed to continuous proliferation. When cells were stained with trypan blue after 7 days in culture both and TCP samples, it was observed that for control groups, there was not a single cells stained blue whereas, 5 (TCP) cells/observed area (insignificant) were stained blue which indicated some level of death in cells which were grown in the presence of β-TCP (Fig. 7b and c).

4. Discussion

β-TCP is a promising candidate of calcium phosphate group which has capacity to be used in preventive and restorative dentistry [5]. Such clinical applications require certain sophisticated features in dental materials such as guided regeneration of tooth tissue needs a material with superior degradability (higher surface area) to assist the osteogenesis process. In present study, we have successfully

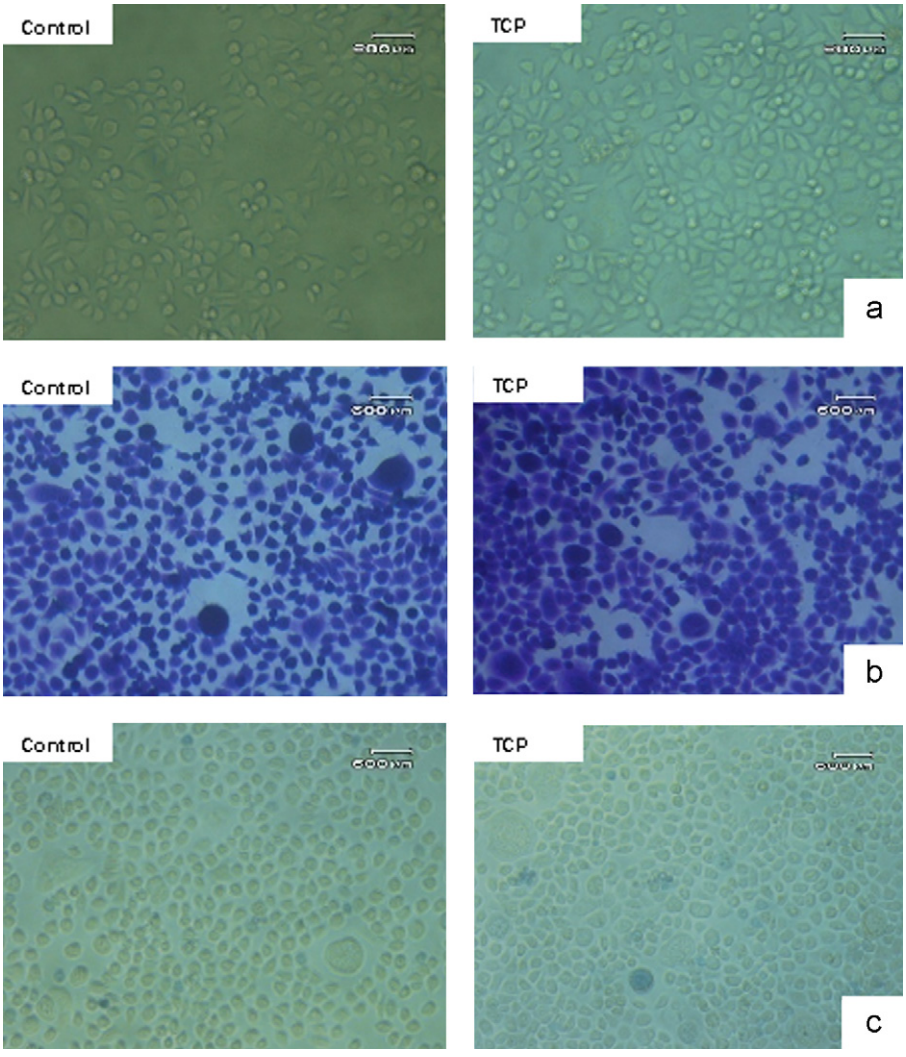

Fig. 7. (a) Bright field images of SF767 cells taken after 7 days of growth (b) Images of SF767 cells after Crystal Violet Staining (C.V); (c) Images of SF767 cells after trypan blue staining.

extended our microwave assisted approach to synthesize nano-scale TCP using CTAB as surfactant. As-precipitated CDA is essentially amorphous in nature. Although it has the high surface area, it is not suitable for the final application. Therefore, the purpose of heat treatment (400 °C–1000 °C) was to study the CDA to β-TCP transformation. As the temperature of heat treatment increases, atoms within a crystal rearrange themselves and crystallinity improves. However, expose surface area is decreased due to closer packing of atoms. Conversion of CDA to β-TCP in the range 600 °C–700 °C was clearly verified by FTIR, XRD and TGA. Further increase in temperature beyond 800 °C resulted in oversize particles (agglomeration) as it seen in the SEM images. Hence it is concluded that transformation to β-TCP is complete at 700 °C and there is no need for higher temperature treatment.

Nanoscale β-TCP was synthesized via microwave assisted technique where the spherical morphology was induced using nonionic surfactant CTAB. CTAB is thought as to evolve micelle in the reaction mixture which acts as potential sites for the nucleation of nanostructures [21]. Spherical morphology is desired for a number of reasons. Firstly, spherical particles have large surface areas for superior binding properties with other materials. Secondly, they exhibit better mechanical properties due to greater chance of close packing of individual particles. The results of the present study show that the nano structure of β-TCP enables more attachment and proliferation of cells thus becoming more biocompatible. This may be due to the nanostructures could provide denser surface, thus higher surface energy to promote initial attachment and spreading of cells [24]. The nanostructures also have enhanced interfacial adhesion to cells and high surface area per volume for cell growth, which might result in increased cellular adherence and proliferation [25]. As discussed earlier, CTAB can assist the formation of spherical nanoparticles. However CTAB is known to burnout at 500 °C, therefore it does not seem to have any effect on the cell proliferation/attachment because in the present study, the cell experiments were performed on the β-TCP that was heat treated at 1000 °C.

Osteoblasts HeLa, and SF767 are the three cell lines used in cell culturing studies. HeLa and SF767 are extensively studied cell lines in cancer and other clinical research. β-TCP showed promising results with these cell lines with respect to cell proliferation. In addition, no cell deaths were observed which implies that the material is not toxic for cells. Hence it is concluded that β-TCP has the potential to be used in clinical applications where tissue regeneration/replacement is a vital requirement.

5. Conclusion

Spherical nanoparticles of CDA were successfully synthesized via the microwave irradiation method in shortest period time. The particles showed their conversion to β-TCP at 700 °C. Cell cytotoxicity analysis confirms this material to be biocompatible.

Acknowledgments

The authors would like to thank Mr. Aftab Akram (School of Chemical and Materials Engineering, National University of Sciences Technology, Islamabad) for his technical support in SEM.

References

[1] R.Z. Le Geros, Properties of osteoconductive biomaterials: calcium phosphates, Clinical Orthopaedics and Related Research 395 (2002) 81–98.
[2] L.L. Hench, Bioceramics: from concept to clinic, Journal of the American Ceramic Society 74 (1991) 510–1487.
[3] P. Ducheyne, S. Radin, L. King, The effect of calcium phosphate ceramic composition and structure on in vitro behavior, Journal of Biomedical Materials Research 27 (1993) 25–34.
[4] J.S. Park, S.J. Hong, H.Y. Kim, H.S. Yu, Y.I. Lee, C.H. Kim, S.J. Kwak, J.H. Jang, J.K. Hyun, H.W. Kim, Evacuated calcium phosphate spherical microcarriers for bone regeneration, Tissue Engineering Part A 16 (2010) 91–1681.
[5] R.Z. Legeros, Calcium phosphate materials in restorative dentistry: a review, Advances in Dental Research 2 (1988) 164–180.
[6] A. Mortier, J. Lemaitre, P.G. Rouxhet, Temperature-programmed characterization of synthetic calcium-deficient phosphate apatites, Thermochimica Acta 143 (1989) 265–282.
[7] P. Kasten, R. Luginbuhl, V. Griensven, T. Barkhausen, C. Krettek, M. Bohner, U. Bosch, Comparison of human bone marrow stromal cells seeded on calcium-deficient hydroxyapatite, β-tricalcium phosphate and demineralized bone matrix, Biomaterials 24 (2003) 2593–2603.
[8] A. Mortier, J. Lemaitre, L. Rodrique, P.G. Rouxhet, Synthesis and thermal behavior of well-crystallized calcium-deficient phosphate apatite, Journal of Solid State Chemistry 78 (1989) 215–219.
[9] I. Teoreanu, M. Preda, A. Melinescu, Synthesis and characterization of hydroxyapatite by microwave heating using $CaSO_42H_2O$ and $Ca(OH)_2$ as calcium source, Journal of Materials Science: Materials in Medicine 19 (2008) 517–523.
[10] A.S. Khan, Z. Ahmed, M.J. Edirisinghe, F.S.L. Wong, I.U. Rehman, Preparation and characterization of a novel bioactive restorative composite based on covalently coupled polyurethane–nanohydroxyapatite fibres, Acta Biomaterialia 4 (2008) 1275–1287.
[11] A.A. Chaudhry, H. Yan, K. Gong, F. Inam, G. Viola, M.J. Reece, J.B.M. Goodall, I. Rehman, F.K. McNeil-Watson, J.C.W. Corbett, J.C. Knowles, J.A. Darr, High-strength nanograined and translucent hydroxyapatite monoliths via continuous hydrothermal synthesis and optimized spark plasma sintering, Acta Biomaterialia 7 (2011) 791–799.
[12] S. Das, A.K. Mukhopadhyay, S. Datta, D. Basu, Prospects of microwave processing: an overview, Bulletin of Materials Science 32 (2009) 1–13.
[13] A. Siddarthan, S.K. Seshadri, T.S. Sampath Kumar, Microwave accelerated synthesis of nanosized calcium deficient hydroxyapatite, Journal of Materials Science: Materials in Medicine 15 (2004) 1279–1284.
[14] A. Farzadi, M. Solati-Hashjin, F. Bakhshi, A. Aminian, Synthesis and characterization of hydroxyapatite/b-tricalcium phosphate nanocomposites using microwave irradiation, Ceramics International 37 (2011) 65–71.
[15] P. Parhi, A. Ramanan, A.R. Ray, A convenient route for the synthesis of hydroxyapatite through a novel microwave-mediated metathesis reaction, Materials Letters 58 (2004) 3610–3612.
[16] D. Chen, X. Qiao, J. Chen, R. Jiang, Convenient, rapid synthesis of silver nanocubes and nanowires via microwave-assisted polyol method, Nanotechnology 21 (2010) 025607–025614.

[17] M.G. Ma, Y.J. Zhu, G.F. Cheng, Y.H. Huang, Microwave synthesis and characterization of ZnO with various morphologies, Materials Letters 62 (2008) 507–510.
[18] Y. Jiang, Y.J. Zhu, Z.L. Xu, Rapid synthesis of Bi_2S_3 nanocrystals with different morphologies by microwave heating, Materials Letters 60 (2006) 2294–2298.
[19] A. Banerjee, A. Bandyopadhyay, S. Bose, Hydroxyapatite nanopowders: synthesis, densification and cell–materials interaction, Materials Science and Engineering C 27 (2007) 729–735.
[20] M.J. Phillips, J.A. Darr, Z.B. Luklinska, I. Rehman, Synthesis and characterization of nano-biomaterials with potential osteological applications, Journal of Materials Science: Materials in Medicine 14 (2003) 875–882.
[21] J.M. Coelho, J. Agostinho Moreira, A. Almeida, F.J. Monteiro, Synthesis and characterization of HAp nanorods from a cationic surfactant template method, Journal of Materials Science: Materials in Medicine 21 (2010) 2543–2549.
[22] X.Y. Lin, H.S. Fan, X.D. Li1a, M. Tang, X.D. Zhang, Evaluation of bioactivity and cytocompatibility of nano-hydroxyapatite/collagen composite in vitro, Bioceramics 17 (2005) 553–556.
[23] M.V. Chaikina, I.A. Khulosov, I.V. Karlo, K.S. Paichadze, Mechanochemical synthesis of nonstiochiometric and substituted apatites with nanosized particles for use as biologically compatible materials, Chemistry for Sustainable Development 12 (2004) 385–394.
[24] H. Li, K.A. Khor, V. Chow, P. Cheang, Nanostructural characteristics, mechanical properties, and osteoblast response of spark plasma sintered hydroxyapatite, Journal of Biomedical Research 82A (2007) 296–303 Part A.
[25] Z. Shi, X. Huang, Y. Cai, R. Tang, D. Yang, Size effect of hydroxyapatite nanoparticles on proliferation and apoptosis of osteoblast-like cells, Acta Biomaterialia 5 (2009) 338–345.